

INFLUENCE OF DIELECTRIC MATERIALS ON IN-VEHICLE ELECTROMAGNETIC FIELDS

A.R. Ruddle

Advanced Engineering Department, MIRA Limited
Watling Street, Nuneaton, Warwickshire, CV10 0TU, UK
E-mail: alastair.ruddle@mira.co.uk; Fax: +44 (0)24 7635 8551

Keywords: Dielectric, electromagnetic field, simulation, vehicle.

Abstract

Numerical simulations and analytical models have been used to investigate the possible impact of various dielectric components of vehicles on internal electromagnetic field distributions. It is found that, apart from the window glazing, the dielectrics investigated have little impact on the internal field populations and average field levels, although there are localized field differences that become more pronounced at higher frequencies. Above 1 GHz typical vehicle glazing panels may increase average field levels for internal sources. However, the windscreen may also reduce the field coupled into the interior under horizontal plane wave illumination from the front of the vehicle at lower frequencies.

1 Introduction

Mathematical modelling is an increasingly popular approach for investigating electromagnetic performance issues in complex environments. Possible application areas include the analysis of radio propagation issues, installed antenna performance, electromagnetic compatibility threats and human exposure to electromagnetic fields. However, as all models of real-world systems inevitably involve a high degree of approximation, it is important to have an understanding of what can reasonably be neglected in the models, under what circumstances, and what the implications may be.

In many cases electromagnetic models of complex systems neglect the various dielectric components that are usually present in the complete system. In a car, for example, components such as the window glazing, seat cushions, dashboard, carpets and other internal trim are often omitted. The motivations for this include:

- model complexity and computing requirements;
- availability of geometry for dielectric components;
- availability of data for their electrical properties.

In all numerical modelling techniques the inclusion of dielectric materials requires additional or denser mesh, and for some methods the associated computational cost can be very significant. Consequently, a metal-only vehicle model is simpler and more efficient, and could perhaps be justified on the grounds that it also provides a “worst-case” configuration.

For example, it has been reported that simulations based on a metal-only vehicle over-estimate the measured internal field by around 6 dB for an on-board GSM antenna operating at around 900 MHz [4]. A further argument for neglecting the dielectric parts at lower frequencies is that they are often electrically thin, and are therefore effectively transparent. Validation studies based on metal-only car models show good correlations with measurements on complete vehicles for frequencies up to 1 GHz [7, 8]. In addition, comparative measurements up to 1 GHz [6] also show relatively small differences due to dielectric parts that are easily removed.

Advances in computing technology and simulation techniques continue to make more sophisticated models increasingly feasible. However, the availability of geometrical data and electrical properties for dielectric components persists as a practical limitation. Thus, there is a need to investigate behaviour at higher frequencies, in order to establish whether dielectric parts may have a greater impact that needs to be taken into account in electromagnetic models.

Simulations of field distributions inside trains [2] and aircraft [5] have been carried out using 3D numerical models that include representations of the internal furnishing. In [5] the effect of removing the furnishings from the aircraft model has been investigated. However, it is important to differentiate the conducting parts of internal furnishings from their dielectric components. Although the conducting parts of structures such as seats do have a significant impact on internal field distributions, the associated dielectric parts have little effect below 1 GHz [6, 11].

A passenger car is sufficiently compact for comparison of a number of simulations, each based on slightly different model variants, to be practicable up to 2 GHz with models that include dielectric materials. Numerical and analytical models have therefore been used to investigate the likely impact of representative dielectric materials on the electromagnetic field distributions inside the passenger compartment of a car. The results obtained may also be of relevance for models of larger vehicles, including ships, trains and aircraft, as well as to other resonant environments such as buildings.

2 Numerical models

In order to investigate the impact of typical vehicle trim materials, a series of staged numerical models was constructed, with material content as follows:

- metal only (case A);
- metal and glass (case B);
- metal, glass and foam (case C);
- metal, glass, foam and thin plastics (case D).

The simulations were carried out using a full-wave 3D transmission line matrix field solver (Microstripes [3]), and the numerical models were derived from 3D geometry for a passenger car. In this study, the impact of the dielectrics is evaluated in terms of the spatial field distribution over the region of the passenger compartment where the occupants may be located. Spatial field data was extracted from the models at more than two million points at selected frequencies up to 2 GHz for this purpose.

The relative permittivity (ϵ_R) and electrical conductivity (σ_E) that were used to represent the different material types are detailed in Table 1, based on samples measured at 3 GHz [10], along with their physical thickness.

| Model feature | Dielectric component | ϵ_R | σ_E (S/m) | Thickness (mm) |
|---------------|----------------------|--------------|------------------|------------------------------|
| Glass | window panels | 6.5 | 0.0325 | windscreen – 5 others - 3 |
| Foam | seats and headrests | 1.14 | 0.0002 | bulk material |
| Plastics | dashboard | 2.46 | 0.0025 | 1–5 |
| | door skins | 2.86 | 0.0029 | 2.5 |
| | B-pillar trim | 2.12 | 0.0003 | 2.2 |

Table 1: Dielectric properties used in vehicle models.

3 Impact on field populations

Simple calculations based on the transmittance of a simple slab of lossless dielectric material illuminated at normal incidence suggest that for typical car window dimensions (ie. 3–6 mm thick) the glazing is effectively transparent for frequencies below 1 GHz. At higher frequencies, however, the thickness can become resonant, resulting in much higher reflections at some frequencies (see Figure 1), depending on materials and construction. Nonetheless, field coupling into the passenger compartment at lower frequencies may also be radically different for horizontally and vertically polarized external plane wave sources at non-normal incidence.

This is illustrated in Fig. 2, which shows the reflectance for a lossless planar dielectric slab under illumination at angles of incidence ranging from 0° (normal incidence) up to 60° (representing a windscreen illuminated from the front by a distance source). In the latter case the reflectance for a horizontally polarized source is around 5% at 1 GHz, rising to more than 25% at 2 GHz, while for vertical polarization the reflectance is negligible. The resulting impact for the internal field populations obtained from the car models is illustrated in Figure 3, where the presence of the glazing clearly reduces the peak of the distribution for horizontal polarization, while the results for vertical polarization show no similar effect (see Figure 4). However, the foam and plastic materials do not have a significant impact on the field populations.

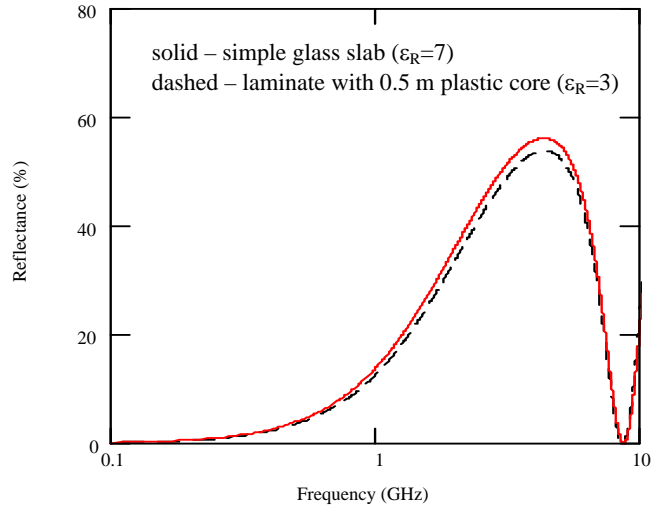
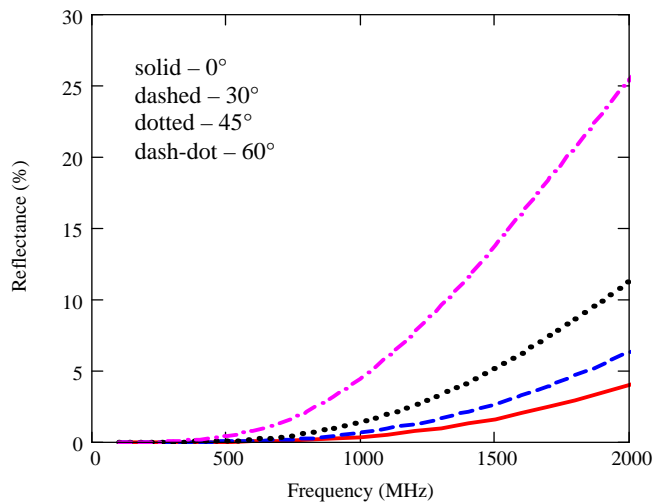
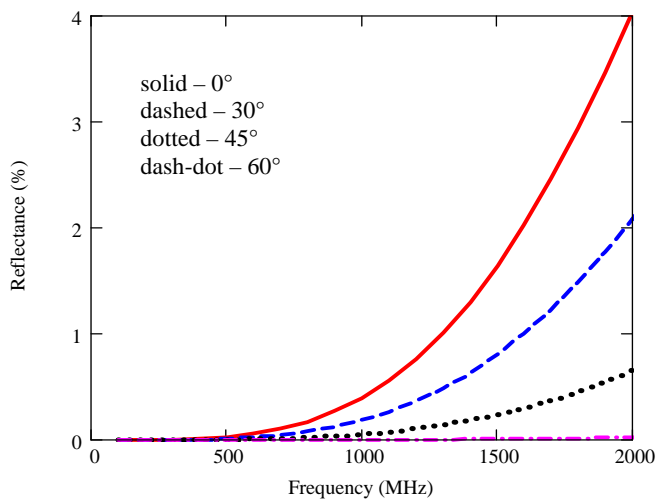


Figure 1: Reflectance of 6.5 mm thick infinite dielectric slab under plane wave illumination at normal incidence



(a) Horizontal polarization



(b) Vertical polarization

Figure 2: Frequency dependence of reflectance for 5 mm thick lossless slab of relative permittivity 6 under plane wave illumination at various angles of incidence.

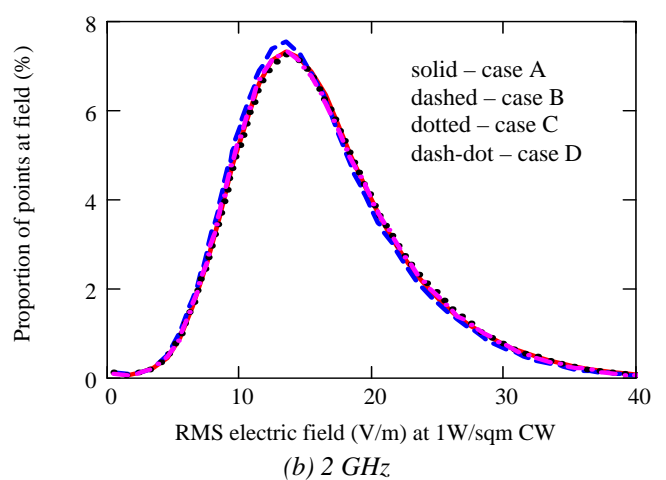
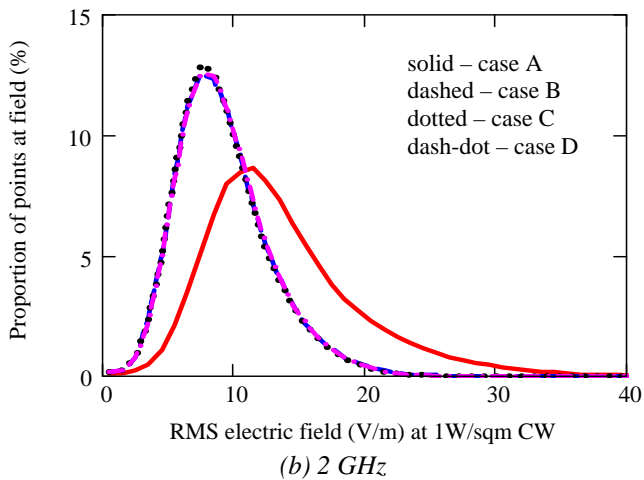
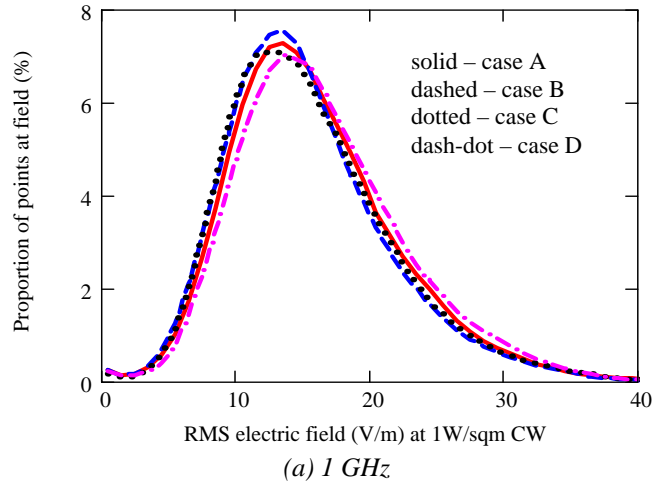
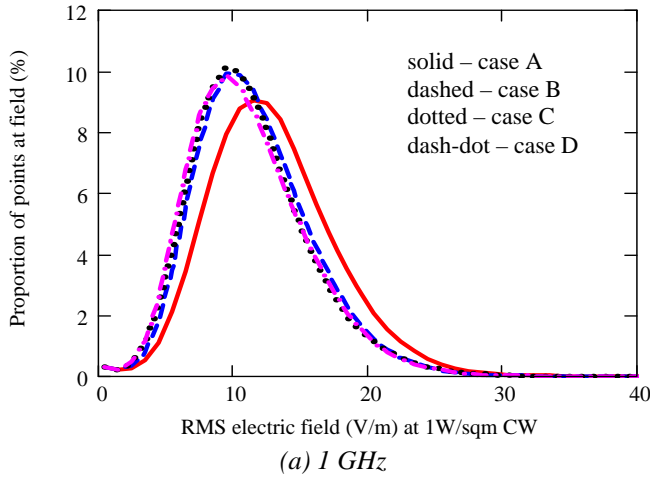


Figure 3: Amplitude distributions for electric field over passenger compartment of car illuminated with horizontal plane wave of 1 W/m^2 power density incident from front.

Figure 4: Amplitude distributions for electric field over passenger compartment of car illuminated with vertical plane wave of 1 W/m^2 power density incident from front.

Internal sources have also been investigated, using simple horizontal and vertical dipole antennas located in the vicinity of the rear seat. In this case (see Figures 5–6) there is not a significant difference between the two source polarizations, and neither the glass nor the foam and plastic materials have a significant impact on the field populations.

4 Impact on average field levels

Average internal electric fields obtained under external plane wave illumination from the front of the car are summarized in Tables 1–2 (for an incident power density of 1 W/m^2). These results show a clear difference between the two polarizations. This is due in part to the differences in coupling through the glass outlined in section 3, but also reflects differences in the response of the metal vehicle structure to the two polarizations, which reduce as the frequency increases (see Table 3). Apart from these effects, however, the average field values are largely unaffected by the additional dielectric content of the models.

| Model case | Average RMS electric field (V/m) at 1 W/m^2 CW | | | | | |
|------------|--|---------|----------|----------|----------|----------|
| | 70 MHz | 400 MHz | 1000 MHz | 1400 MHz | 1800 MHz | 2000 MHz |
| A | 17.32 | 14.19 | 15.99 | 16.68 | 16.78 | 16.19 |
| B | 19.05 | 13.15 | 15.41 | 16.27 | 16.67 | 15.82 |
| C | 19.23 | 13.32 | 15.63 | 15.92 | 16.16 | 16.24 |
| D | 20.44 | 13.16 | 16.55 | 16.25 | 16.12 | 16.12 |

Table 1: Average internal electric fields for car models under 1 W/m^2 horizontal plane wave illumination from front.

| Model case | Average RMS electric field (V/m) at 1 W/m^2 CW | | | | | |
|------------|--|---------|----------|----------|----------|----------|
| | 70 MHz | 400 MHz | 1000 MHz | 1400 MHz | 1800 MHz | 2000 MHz |
| A | 1.32 | 12.51 | 12.97 | 14.01 | 13.92 | 13.76 |
| B | 1.41 | 11.91 | 11.63 | 10.64 | 9.63 | 9.27 |
| C | 1.41 | 11.55 | 11.28 | 9.95 | 9.41 | 9.16 |
| D | 1.55 | 13.32 | 11.22 | 10.40 | 9.78 | 9.28 |

Table 2: Average internal electric fields for car models under 1 W/m^2 vertical plane wave illumination from front.

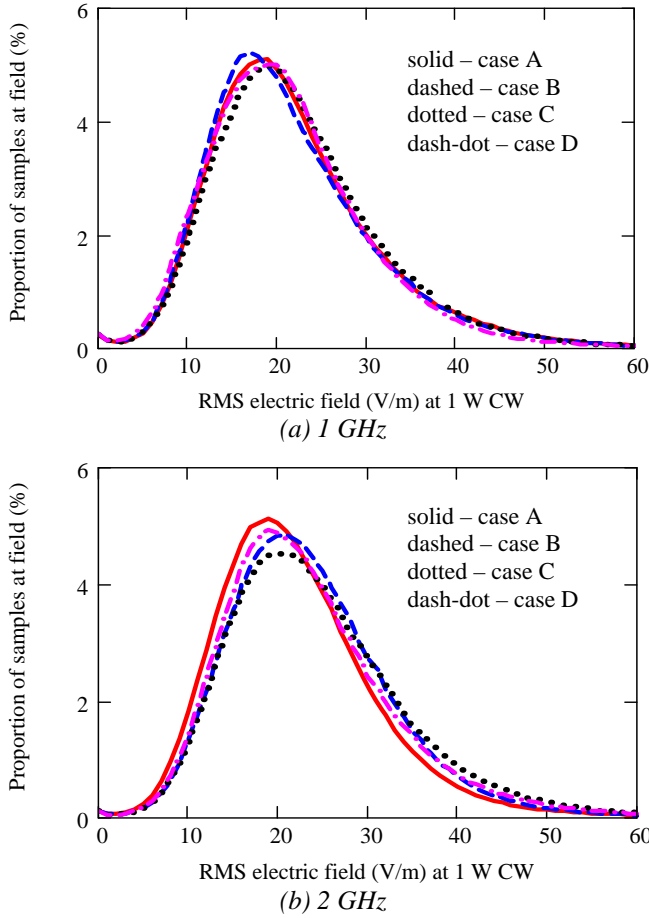


Figure 5: Amplitude distributions for electric field over passenger compartment of car with internal horizontal dipole source at 1 W radiated power.

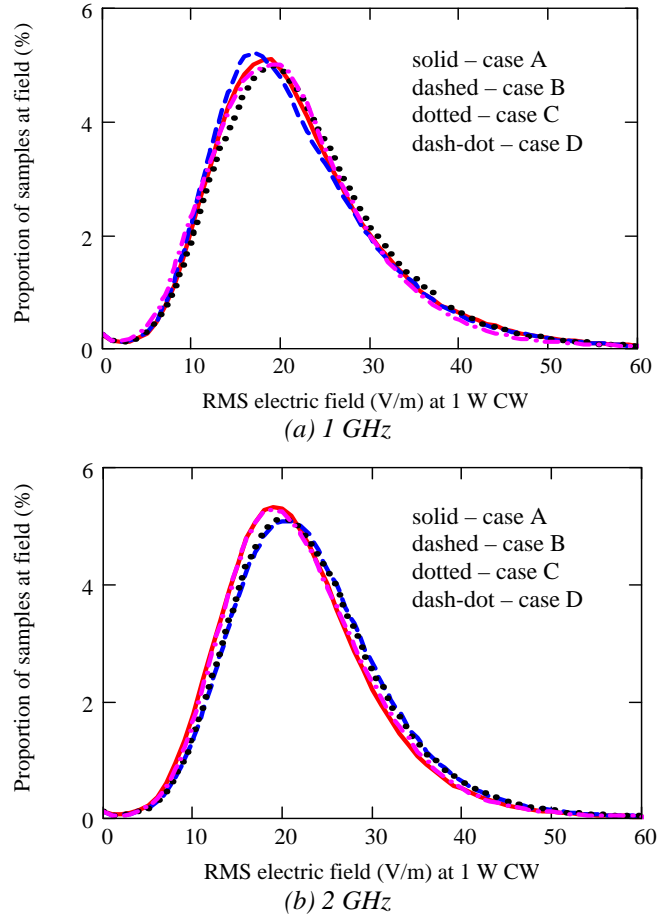


Figure 6: Amplitude distributions for electric field over passenger compartment of car with internal vertical dipole source at 1 W radiated power.

| Source case | Average RMS electric field (V/m) at 1 W/m ² CW | | | | | |
|-------------|---|----------|----------|----------|----------|----------|
| | 400 MHz | 1000 MHz | 1400 MHz | 2000 MHz | 2400 MHz | 3000 MHz |
| V | 14.19 | 15.99 | 16.68 | 16.19 | 15.16 | 13.20 |
| H | 12.51 | 12.97 | 14.01 | 13.76 | 13.68 | 13.48 |

Table 3: Average internal electric fields for car model without dielectrics under 1 W/m² plane wave illumination from front.

For the internal dipole sources (see Table 4), the average internal electric fields are also largely unaffected by the presence of dielectric materials in the models, although the impact of the glass is becoming more apparent in the 2 GHz data. This is also expected from simple analytical models.

| Model case | Average RMS electric field (V/m) at 1 W CW | | | | | |
|------------|--|-------|---------|-------|-------|-------|
| | 1 GHz | | 1.5 GHz | | 2 GHz | |
| | V | H | V | H | V | H |
| A | 22.30 | 22.72 | 23.30 | 24.30 | 22.52 | 22.89 |
| B | 21.79 | 22.39 | 23.89 | 24.35 | 23.69 | 24.43 |
| C | 22.69 | 23.03 | 24.44 | 23.06 | 23.59 | 25.41 |
| D | 22.63 | 22.00 | 23.28 | 22.92 | 22.71 | 24.18 |

Table 4: Average internal electric fields for 1 W vertical and horizontal dipoles located inside car passenger compartment.

Above 1 GHz the vehicle interior is sufficiently large (relative to the wavelength) to exploit power balance methods [1] in order to estimate the average internal field strengths and population distributions from very limited geometrical data.

Assuming that the windows represent the dominant source of loss for the system, and that they are also electrically large at the frequencies of interest, the average field strength can be estimated from the window areas, glazing construction and the power coupled into the vehicle interior [9]. For windows of area A_k , the RMS electric field strength averaged over the volume of the cavity at frequency f is approximately:

$$\langle E_{RMS}(f) \rangle \approx \sqrt{\frac{240\pi}{\sum_k \left[\frac{A_k}{2} w_k(f) \right]}} P_R(f) \quad (1)$$

where $P_R(f)$ is the power coupled into the interior and the $w_k(f)$ are frequency dependent aperture weighting factors that represent the properties of the glazing used in each window k . These aperture weighting factors are determined [9] from:

$$w_k(f) = \int_0^{\pi/2} [T_{k\perp}(f, \theta) + T_{k\parallel}(f, \theta)] \cos(\theta) \sin(\theta) d\theta \quad (2)$$

where $T_{k\perp}(f, \theta)$ and $T_{k\parallel}(f, \theta)$ represent the transmittances for the glazing panel in aperture k with the incident field polarizations perpendicular and parallel to the plane of incidence, respectively, and θ is the angle of incidence.

Using these analytical approximations it is possible to predict the average internal electric field strengths due to internal sources at microwave frequencies (see Fig. 7) for vehicles with various glazing configurations. These very simple estimates are found to compare well with average field values derived from detailed 3D numerical models (see Fig. 8).

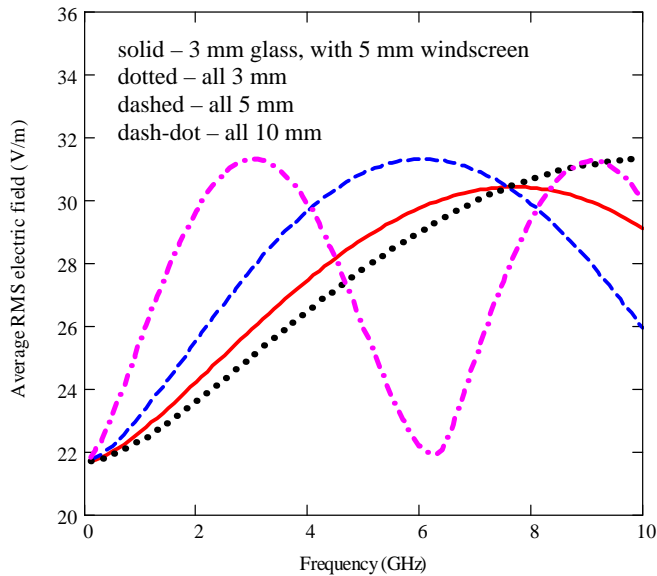


Figure 7: Estimated average internal electric field for car with 1 W internal source for various glazing configurations based on a single layer of lossless glass.

5 Local differences due to dielectrics

The cumulative distributions for relative errors between the metal only model and those with different dielectric content give an indication of the impact of these materials on local field levels. Sample results for external vertical plane wave illumination are illustrated in Figs. 9–10, showing that the differences rise from less than 40% at 70 MHz to more than 100% at 400 MHz. Sample results for an internal horizontal source at 1–2 GHz (Figs. 11–12) also indicate that the local differences continue to increase at higher frequencies.

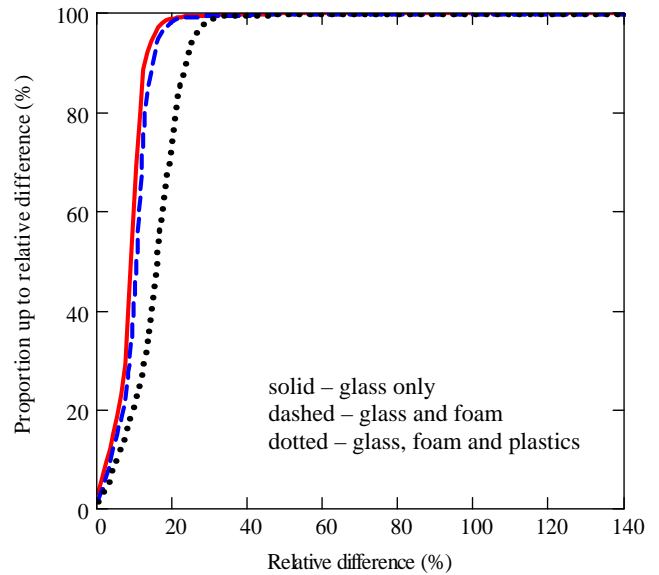


Figure 9: Cumulative distribution of relative differences due to dielectric materials under vertical plane wave illumination from front at 70 MHz.

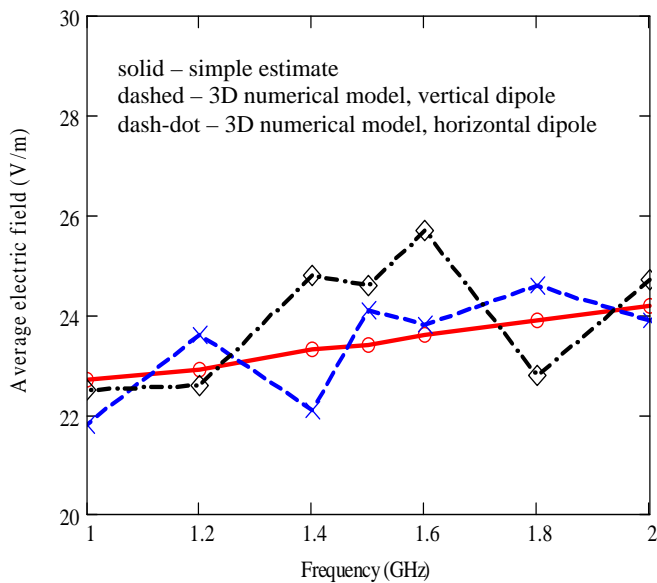


Figure 8: Comparison of simple estimates for average internal electric field strength with detailed 3D numerical models for 3 mm glass with 5 mm windscreen with 1 W internal sources.

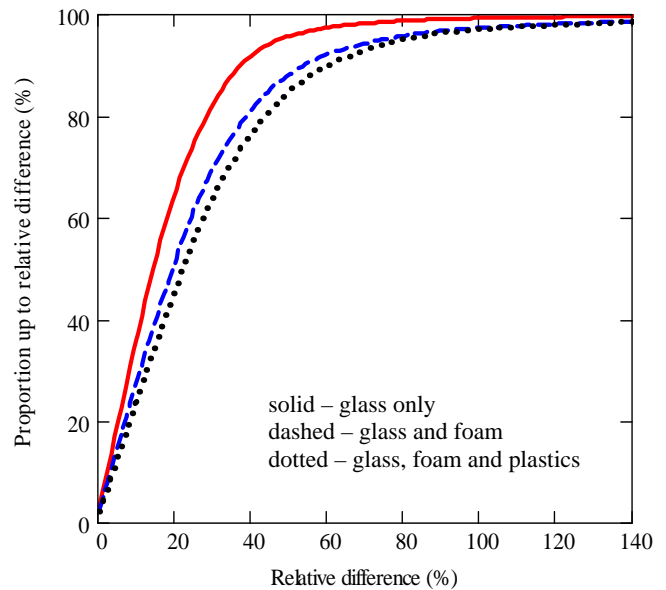


Figure 10: Cumulative distribution of relative differences due to dielectric materials under vertical plane wave illumination from front at 400 MHz.

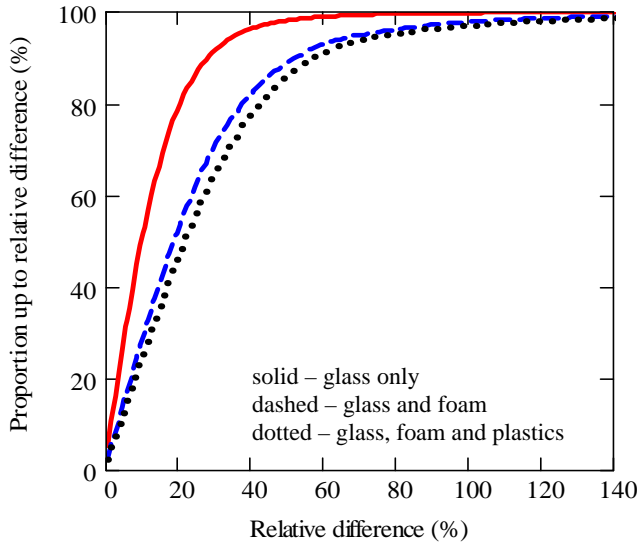


Figure 11: Cumulative distribution of relative differences due to dielectric materials for internal horizontal dipole at 1 GHz.

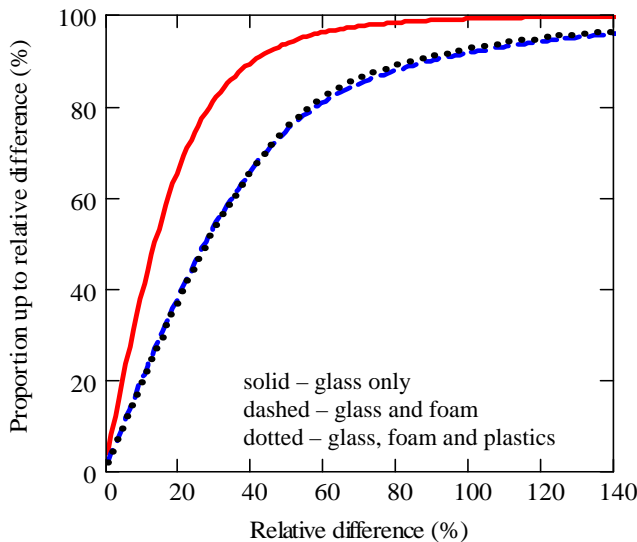


Figure 12: Cumulative distribution of relative differences due to dielectric materials for internal horizontal dipole at 2 GHz.

6 Conclusions

Simple analytical models suggest that car window glazing is likely to become increasingly important for in-vehicle fields at frequencies above 1 GHz, and may be significant for some external plane wave illumination configurations at lower frequencies. Numerical models based on 3D vehicle geometry also support these conclusions. In addition, the results of the 3D simulations indicate that foam and plastic materials found in the interiors of passenger cars do not have a significant impact on the statistical properties of the internal field distributions, for frequencies up to 2 GHz. Nonetheless, the simulations suggest that the presence of dielectric materials can result in significant changes in the local field strength at individual points (with relative differences of >100%), and that these changes become greater at higher frequencies.

Acknowledgements

The work outlined above was carried out as part of SEFERE (see www.sefere.org), a collaborative research project that is supported by the UK's Technology Strategy Board (contract TP/3/DSM/6/I/15266) and Engineering and Physical Sciences Research Council (grant EP/D033187/1). The project consortium includes MIRA Limited (coordinator), ARUP Communications, BAE Systems, Harada Industries Europe, Jaguar Cars, University of Sheffield, UK National Policing Improvements Agency and Volvo Car Corporation (Sweden).

References

- [1] D.A. Hill, M.T. Ma, A.R. Ondrejka, B.F. Riddle, M.L. Crawford and R.T. Johnk, "Aperture excitation of electrically large, lossy cavities", *IEEE Trans. EMC*, **Vol. 36**(3), pp. 169–178, (1994).
- [2] M. Hirono, T. Hikage, Y. Abiko, T. Nojima, S. Watanabe and T. Shinozuka, "Large-scale parallel FDTD analysis of electromagnetic fields (EMF) excited with cellular phones in actual train carriages", *Proc. 7th European Symposium on EMC*, Barcelona, Spain, pp. 486–491, (2006).
- [3] D.P. Johns, R. Scaramuzza and A.J. Wlodarczyk, "Micro-Stripes – microwave design tool based on 3D-TLM", *Proc. 1st International Workshop on Transmission Line Matrix (TLM) Modeling – Theory and Applications*, Victoria, Canada, pp. 169–177, (1995).
- [4] M. Klingler and A. Lecca, "Comparison between simulations and measurements of the fields created by a mounted GSM antenna using a car body instead of an entire vehicle", *Proc. 7th European Symposium on EMC*, Barcelona, Spain, pp. 732–742, (2006).
- [5] E. Perrin, F. Tristant, S. Gouverneur, R. Fayat, C. Guiffaut, A. Reineix and J.-P. Moreau, "Study of electric field radiated by WiFi sources inside an aircraft – 3D computations and real tests", *Proc. 8th European Symposium on EMC*, Hamburg, Germany, pp. 313–317, (2008).
- [6] A.R. Ruddle, "Measured impact of vehicle seats and glazing on the coupling of electromagnetic fields into vehicles and their wiring harnesses", *Proc. 15th Int. Zurich EMC Symposium*, Zurich, Switzerland, pp. 487–492, (2003).
- [7] A.R. Ruddle, X. Ferrières, J.-P. Parmantier and D.D. Ward, "Experimental validation of time-domain electromagnetic models for field coupling into the interior of a vehicle due to a nearby broadband antenna", *IEE Proc. Science, Measurement and Technology*, **Vol. 151**(6), pp. 430–433, (2004).
- [8] A.R. Ruddle, "Validation of predicted 3D electromagnetic field distributions due to vehicle mounted antennas against measured 2D external electric field mapping", *IET Science, Measurement and Technology*, **Vol. 1**(1), pp. 71–75, (2007).
- [9] A.R. Ruddle, "Simple estimation of average field strengths in resonant environments for assessing human exposure to electromagnetic fields", *Proc. 8th European Symposium on EMC*, Hamburg, Germany, pp. 209–214, (2008).
- [10] A.R. Ruddle, H. Zhang, L. Low, J. Rigelsford, and R.J. Langley, "Numerical investigation of the impact of dielectric components on electromagnetic field distributions in the passenger compartment of a vehicle", to be published in *Proc. 20th Int. Zurich EMC Symposium*, Zurich, Switzerland, (2009).
- [11] H. Zhang, J. Rigelsford, L. Low, and R.J. Langley, "Field distributions within a rectangular cavity with vehicle-like features", *Proc. 2008 Loughborough Antennas and Propagation Conf.*, Loughborough, UK, pp. 205–208, (2008).